Magnetization, persistent currents, and their relation in quantum rings and dots

W.-C. Tan and J. C. Inkson
School of Physics, University of Exeter, Stocker Road, Exeter EX4 4QL, United Kingdom
(Received 16 December 1998)

An exactly soluble model is used to study magnetization and persistent currents of electrons confined in two-dimensional mesoscopic rings and dots. The model allows the calculation of magnetization and persistent currents for a range of device geometries containing a large number of electrons ($>10^3$) with little computational requirement. It is shown that in the weak-magnetic-field limit, the persistent current is simply proportional to the magnetization, presenting Aharonov-Bohm (AB) type oscillations. Such oscillations are aperiodic due to the penetration of magnetic field into the conducting region. In the strong-magnetic-field regime, however, the persistent currents and the magnetization have very different behaviors. While the persistent currents still show a rapid AB-type oscillation, the magnetization is dominated by de Haas–van Alphen (dHvA) type oscillations with the much weaker AB-type oscillations superimposed on them. The effect of device geometry on the persistent current is also very different from that on magnetization. Both the oscillation amplitude and the period of the persistent current are very sensitive to the device geometry, while the magnetization in different devices shows very similar dHvA-type oscillations. Our calculated typical value of weak-magnetic-field persistent current in a semiconductor ring, 4.95 nA, is in very good agreement with the experimental result of Mailly, Chapelier, and Benoit [Phys. Rev. Lett. **70**, 2020 (1993)]: 4 ± 2 nA.
[S0163-1829(99)10331-X]

I. INTRODUCTION

The recent experimental observation of persistent currents in mesoscopic rings[1–3] has received considerable theoretical attention. One of the most important goals has been to go beyond the one-dimensional picture of persistent currents[4,5] and to study the persistent current in a ring of finite width.[6–9] Because of the difficulty in dealing with a real annular geometry, most theoretical studies have been performed using simple models for narrow rings in weak magnetic fields, in which a ring with a finite width is approximated by more manageable models, such as two-dimensional (2D) or three-dimensional (3D) straight wires with periodic boundary conditions, and a uniform magnetic field is replaced by a thin magnetic flux tube confined to the hole region of the ring.[9–12] Within such simple models, varying the magnetic-field strength only changes the phases of the electrons, resulting in periodic mesoscopic oscillations in the electronic properties [a manifestation of the Aharonov-Bohm (AB) oscillations], and the persistent current (I) in a ring is simply related to the magnetic moment (M) of the ring by $I=M/S$, where S is the area of the ring. These simple models have provided convenient tools for studying more complicated problems such as the effects of electron-electron interaction and disorder scattering on persistent currents. However, the behavior of a real annular ring in a uniform magnetic field can be well beyond the description of such simple models, especially when the magnetic field is strong. For example, the penetration of magnetic field into the conducting region can result in aperiodic oscillations in the persistent currents and the breakdown of the simple linear relation between the persistent current and the magnetization. Since at present the only way to probe persistent currents in mesoscopic rings is by measuring the magnetization, it is highly desirable to gain a complete understanding of the persistent currents, the magnetization, and their relation for a realistic 2D ring over the whole range of magnetic-field strength.

Full quantum-mechanical calculations of persistent currents and magnetization based on numerically solving the Schrödinger equation for a 2D ring in a uniform magnetic field have been reported recently. Avishai, Hatsugai, and Kohmoto[7] calculated persistent currents in a 2D ring defined by a hard-wall confinement potential. They found that in the presence of a strong magnetic field the persistent current has a plateau as a function of electron density when the Fermi energy is locked on a Landau level. Chakraborty and Pietilainen[13] studied the effect of electron-electron interaction on the magnetization by numerically solving the electron states in a 2D ring containing a small number of electrons. However, due to the limitation of computational power, the numbers of electrons considered in these numerical studies are much smaller than those in rings used in actual experiments.[1–3]

Recently we proposed an exactly soluble model potential of a 2D ring.[14] The exact energy spectrum and wave functions are obtained analytically for the model for the case of a uniform perpendicular magnetic field and a thin magnetic flux confined to the ring center. The model has been successfully used to explain beating in the AB oscillations experimentally observed in 2D semiconductor rings.[15–17] In the present paper we use this model to study persistent currents and magnetization in 2D rings and dots. We have derived exact expressions for both the magnetic moment and the current carried by an electron state, which enables the calculation of magnetization and persistent currents for rings containing a large number of electrons with a minimum of computational power. Without using this model such a calculation could be very computationally demanding if not impossible.

In order to provide a complete picture for the relation

between the magnetization and persistent currents in 2D rings and disks, we have calculated both the persistent currents and the magnetization over a wide range of magnetic-field strength for rings with different width to radius ratios. Since the main purpose of this paper is to study the effects of device geometry on the persistent currents, the magnetization, and their relationship, we have confined ourselves to an independent spinless electron model. In the low-magnetic-field regime ($B<10^{-2}$ T), the spinless independent electron model should be a good approximation for the semiconductor structures considered here, which have an electron density higher than 3.5×10^{11} cm^{-2}. In this regime, the main effect of electron-electron interaction is a shift of the total energy.[18] Since the Zeeman splitting is very small, the spin degree of freedom just doubles the number of transverse channels in a ring, and therefore its contribution to the persistent currents and magnetization may be included to a good approximation by a factor of $\sqrt{2}$. Consequently one can expect that the simple model can provide an adequate description of experiments on high-quality semiconductor structures performed at low temperature and weak magnetic fields. As an example, in this paper we have calculated the weak-magnetic-field persistent currents in a semiconductor ring which has a similar parameter to the experimental device used in Ref. 3. It is found that our calculated typical value of persistent current is in very good agreement with the experimental result.[3]

In the strong-magnetic-field regime the effects of electron correlation and the spin freedom of the electrons become significant,[18] which is most evident in fractional quantum Hall systems. In quantum dots and rings containing only a few electrons, the electron correlation and the spin freedom of the electrons are important even in the weak-magnetic-field regime.[13,19,20] It has been conjectured that the combination of electron correlation and disorder scattering is the physical origin of the large persistent currents observed in metal rings,[21] but the detailed physical mechanism for the enhanced persistent currents is still an open question. In the present paper we do not attempt to tackle these important problems, such as electron interaction and disorder scattering. However, the exact solutions of our model provide a very useful basis set to study the effect of disorder and electron-electron interaction in quantum rings and dots. Furtermore, even the simple model may lead to results of fair complexity. A thorough understanding of the results of our simple model will assist in the identification of many-body effects and disorder effects in real systems, and therefore pave the way to a complete description of the real systems. For example, in their experiments, Liu *et al.*[16] found that the magnetoresistance of a semiconductor 2D ring as a function of magnetic-field strength exhibited apparently random oscillations when more than one subband is occupied. It was suggested that the random oscillations was due to disorder scattering, but it contradicted the fact that the magnetoresistance of the same ring exhibited well-defined periodic oscillations. A simple calculation using the 2D ring model clearly shown that the apparent random oscillations were due to the penetration of magnetic field into the conducting region of a 2D ring, rather than disorder scattering.[15]

The rest part of the paper is arranged as follows. In Sec. II we describe the 2D ring model and its general solutions. Explicit expressions for both the magnetic moment and the current carried by an electron state are derived. In Sec. III we present numerical results for three devices: a narrow ring, a wide ring, and a dot. The calculated persistent currents for the narrow ring are also compared with the experimental results of Ref. 3. A summary of the results is given in Sec. IV.

II. MODEL AND FORMULATION

We consider noninteracting spinless electrons in a 2D ring defined by a radial potential,[14]

$$V(r)=\frac{a_1}{r^2}+a_2r^2-V_0, \tag{1}$$

where $V_0=2\sqrt{a_1a_2}$. A detailed analysis of this model was given in Ref. 14. The key parameters of this model are as follows: the average radius of the ring is given by $r_0=(a_1/a_2)^{1/4}$, the width of the ring at Fermi energy E_f is $\Delta r\approx\sqrt{8E_f/\mu\omega_0^2}$, where $\omega_0=\sqrt{8a_2/\mu}$; and μ is the electron effective mass. For r near r_0, the potential of the ring is parabolic: $V(r)\approx\frac{1}{2}\mu\omega_0^2(r-r_0)^2$. If we take $a_1=0$, $V(r)$ describes a quantum dot.

In the presence of a uniform perpendicular magnetic field B and an infinite thin magnetic flux $\Phi=l\phi_0$, where $\phi_0=h/e$, piercing through the ring center, the eigenenergies and eigen-wave-functions are[14]

$$E_{n,m}=\left(n+\frac{1}{2}+\frac{M}{2}\right)\hbar\omega-\frac{m-l}{2}\hbar\omega_c-V_0, \tag{2}$$

$$\Psi_{n,m}(r,\theta)=\left(\frac{\Gamma(n+M+1)}{2^{M+1}[\Gamma(M+1)]^2n!\pi}\right)^{1/2}\times\frac{e^{im\theta}r^Me^{-(1/4)(r/\lambda)^2}}{\lambda^{M+1}}{}_1F_1\left(-n,M+1,\frac{1}{2}(r/\lambda)^2\right), \tag{3}$$

$$n=0,1,2,3,\ldots,\quad m=\ldots,-2,-1,0,1,2,\ldots,$$

where

$$\omega_c=\frac{eB}{\mu},\quad \omega=\sqrt{\omega_c^2+\omega_0^2},\quad \lambda=\sqrt{\frac{\hbar}{\mu\omega}},$$

$$M=\sqrt{(m-l)^2+\frac{2a_1\mu}{\hbar^2}}, \tag{4}$$

and ${}_1F_1$ is the hypergeometic function or Kumar function.

At zero temperature, the magnetization of a system containing a fixed number (N) of electron is given by

$$\mathcal{M}(B)=-\left.\frac{\partial U}{\partial B}\right|_N, \tag{5}$$

where

$$U=\sum_{n,m}E_{n,m} \tag{6}$$

is the total energy of the electron system. (The summation is taken over the N occupied states. The electron spin is ignored here.) Apart from a set of zero-measure field values where the magnetization is discontinuos, Eq. (5) may be rewritten as

$$\mathcal{M}(B)=\sum_{n,m}\mathcal{M}_{n,m}(B), \tag{7}$$

where

$$\mathcal{M}_{n,m}(B)=-\left.\frac{\partial E_{n,m}}{\partial B}\right|_{N} \tag{8}$$

is the magnetic moment of the (n,m)th state. Substituting Eq. (2) into Eq. (8) gives the simple result

$$\mathcal{M}_{n,m}=-\frac{\hbar e}{\mu}\left[\left(n+\frac{1}{2}+\frac{M}{2}\right)\frac{\omega_c}{\omega}-\frac{m-l}{2}\right]. \tag{9}$$

Using the definition of the current density operator, the circular current carried by a given electron state $\Psi_{n,m}$ can be calculated by

$$I_{n,m}=\int_0^{2\pi}d\theta\int_0^{\infty}dr\, j_{n,m}(r,\theta), \tag{10}$$

where

$$j_{n,m}(r,\theta)=\frac{e\hbar}{\mu}\Psi^{*}_{n,m}(r,\theta)\left[\frac{1}{r}\left(i\frac{\partial}{\partial\theta}-l\right)-\frac{eBr}{2\hbar}\right]\Psi_{n,m}(r,\theta). \tag{11}$$

However, since we have an analytical expression (2) for the energy spectrum, and the wave functions of the ring states are zero at $r=0$, it is more convenient to calculate $I_{n,m}$ using the Byers-Yang relation[4]

$$I_{n,m}=-\frac{\partial E_{n,m}}{\partial\Phi}=-\frac{1}{\phi_0}\frac{\partial E_{n,m}}{\partial l}. \tag{12}$$

Substituting Eq. (2) into Eq. (12), we obtain

$$I_{n,m}=\frac{e\omega}{4\pi}\left(\frac{m-l}{M}-\frac{\omega_c}{\omega}\right). \tag{13}$$

The total persistent current of the ring is then the summation of the currents carried by all the occupied electron states:

$$I=\sum_{n,m}I_{n,m}. \tag{14}$$

To see the relation between the persistent currents and the magnetization clearly, we rewrite Eq. (9) in the form

$$\mathcal{M}_{n,m}=\pi r_{n,m}^2 I_{n,m}-\frac{e\hbar}{\mu}\left(n+\frac{1}{2}\right)\frac{\omega_c}{\omega}, \tag{15}$$

where $r_{n,m}=\sqrt{2M}\lambda$ is the effective radius of the (n,m)th states.[14] The physical meaning of Eq. (15) is very clear. The first term is the classical magnetic moment of a current loop with a radius $r_{n,m}$. The second term is the diamagnetic shift term, resulting from the magnetic modification of the radial wave function.

It can be seen from Eq. (15) that only in the weak-magnetic-field limit (or equivalently the narrow ring limit), i.e., $\omega_c \ll \omega_0$, is the magnetic moment of an electron state proportional to its current. It should also be noted that, for a state near a subband bottom, $I_{n,m}\approx 0$, and therefore the diamagnetic term always dominates the magnetization. This equation is dependent upon only fairly model-independent parameters: the effective radius, the cyclotron frequency, and the magnetic-field-shifted frequency ω. We would therefore expect the result to have applicability beyond our present model.

All the above results are also valid for electron states in quantum dots where $a_1=0$, except for the states with $m-l=0$. This is because, when $a_1=0$, the wave function of a state with $m-l=0$ has a nonzero value at $r=0$, and the Byers-Yang relation (12) no longer applies. However, since Eq. (13) applies for all states if $a_1\neq 0$, the circular current carried by an $m-l=0$ state in a quantum dot can be obtained by taking the limit

$$I_{n,m}|_{m-l=0}=\lim_{a_1\to 0^{+}}\left[\lim_{m\to l}\frac{e\omega}{4\pi}\left(\frac{m-l}{M}-\frac{\omega_c}{\omega}\right)\right]=-\frac{e\omega_c}{4\pi}. \tag{16}$$

This is exactly the same as the result obtained by Avishai and Kohmoto through evaluating the current density from the wave function. The current carried by an $m\neq l$ state in a parabolically confined quantum dot can be obtained from Eq. (13) by taking $M=|m-l|$:

$$I_{n,m}=\begin{cases}-\dfrac{e(\omega_c-\omega)}{4\pi} & \text{if } m-l>0\\[2ex] -\dfrac{e(\omega_c+\omega)}{4\pi} & \text{if } m-l<0.\end{cases} \tag{17}$$

This tells us that all the clockwise-moving states ($m>l$) contribute exactly the same current, and so do the counterclockwise ($m<l$) moving states. In the strong-magnetic-field limit, $\omega-\omega_c\to 0$, a state with $m-l>0$ carries no current while a state with $m-l<0$ carries a large current $-e\omega_c/2\pi$, which is in turn twice the value of the $m=l$ states. Therefore, at a strong magnetic field, the total persistent current of a quantum dot as a function of electron number is quantized in units of $e\omega_c/4\pi$. Such quantized persistent currents in a quantum dot were first found by Avishai and Kohmoto using a hard-wall confinement potential.[6] They showed that the nonzero currents carried by the $m=0$ states (only the $l=0$ case was discussed in Ref. 6) play an important role in quantized persistent currents in a quantum dot.

III. NUMERICAL RESULTS

Using the model described in Sec. II, we have calculated numerically the magnetization and persistent currents as a function of magnetic field for three devices: a narrow ring ($\hbar\omega_0=2.23$ meV, $r_0=1350$ nm), a wide ring ($\hbar\omega_0=0.734$ meV, $r_0=400$ nm), and a dot ($\hbar\omega_0=0.459$ meV, $r_0=0$), as schematically shown in Fig. 1. In order to compare with experimental results, the parameters of the narrow ring are chosen to be similar to those of the 2D GaAs ring used in the

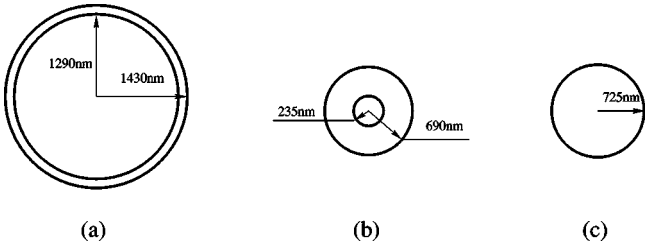

FIG. 1. A schematic illustration of three devices: (a) narrow ring ($\hbar\omega_0=2.23$ meV, $r_0=1350$ nm); (b) a wide ring ($\hbar\omega_0=0.734$ meV, $r_0=400$ nm); and (c) a dot ($\hbar\omega_0=0.459$ meV, $r_0=0$).

persistent current measurement of Ref. 3. Each of the three devices contains $N=1400$ (spinless) electrons. The electron effective mass $\mu=0.067\mu_0$ for GaAs is used. Figure 2 shows the zero-temperature Fermi energies of three device as a function of magnetic-field strengths. It can be seen that at $B=0$ the Fermi energies are about 12.2 meV for all the three devices. All the numerical results presented in this paper are calculated with the assumption of zero temperature and $l=0$ (i.e., there is no AB flux confined to the center of the devices).

A. Persistent currents

Figure 3(a) shows the calculated persistent currents for the narrow ring as a function of magnetic-field strengths. To see clearly the low- and high-field behaviors of the persistent currents, enlargements of the low- and high-field parts of Fig. 3(a) are shown in Figs. 3(b) and 3(c), respectively. The corresponding results for the wide ring and the dot are shown in Figs. 4 and 5. Since the persistent current is antisymmetric about $B=0$, we will only consider the case of $B\geqslant 0$.

We start by looking at the results of the two devices with a ring geometry. It can been seen from Figs. 3(a) and 4(a) that for both narrow and wide rings the persistent currents show rapid oscillations within the whole magnetic range, which reflect the magnetic-field-induced redistribution of electrons in the clockwise- and counterclockwise-moving

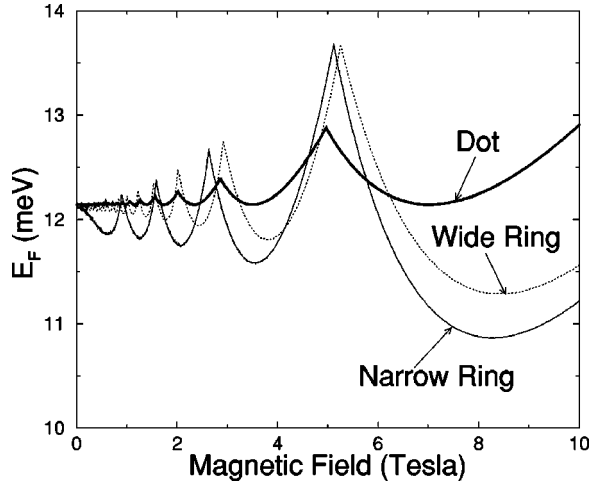

FIG. 2. The zero-temperature Fermi energy as a function of magnetic-field strength for the narrow ring (thin solid line), the wide ring (thick solid line), and the dot (broken line). There are 1400 (spinless) electrons in each device.

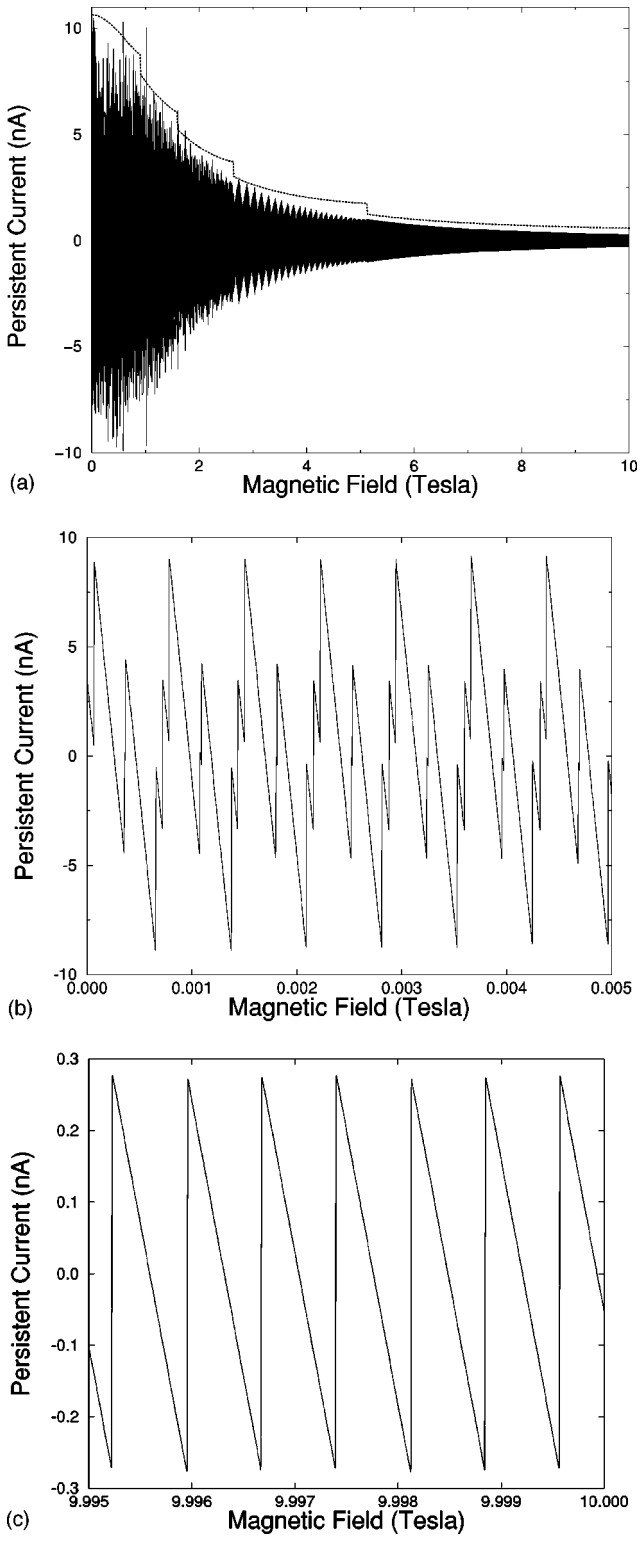

FIG. 3. (a) The persistent currents of the narrow ring as a function of magnetic-field strength obtained from the exact model calculation (real line). The broken line shows the persistent currents calculated with the simple formula (19). (b) and (c) are the enlargements of the weak- and strong-field parts of the exact results shown in (a), respectively.

states in different subbands. Figure 3(b) shows that for the narrow ring the persistent current oscillation pattern in the very weak-magnetic-field region is almost periodic. The period $p_0\approx 0.000\,717$ T corresponds to $\Delta B=p_0=\phi_0(\pi r_0^2)^{-1}$.

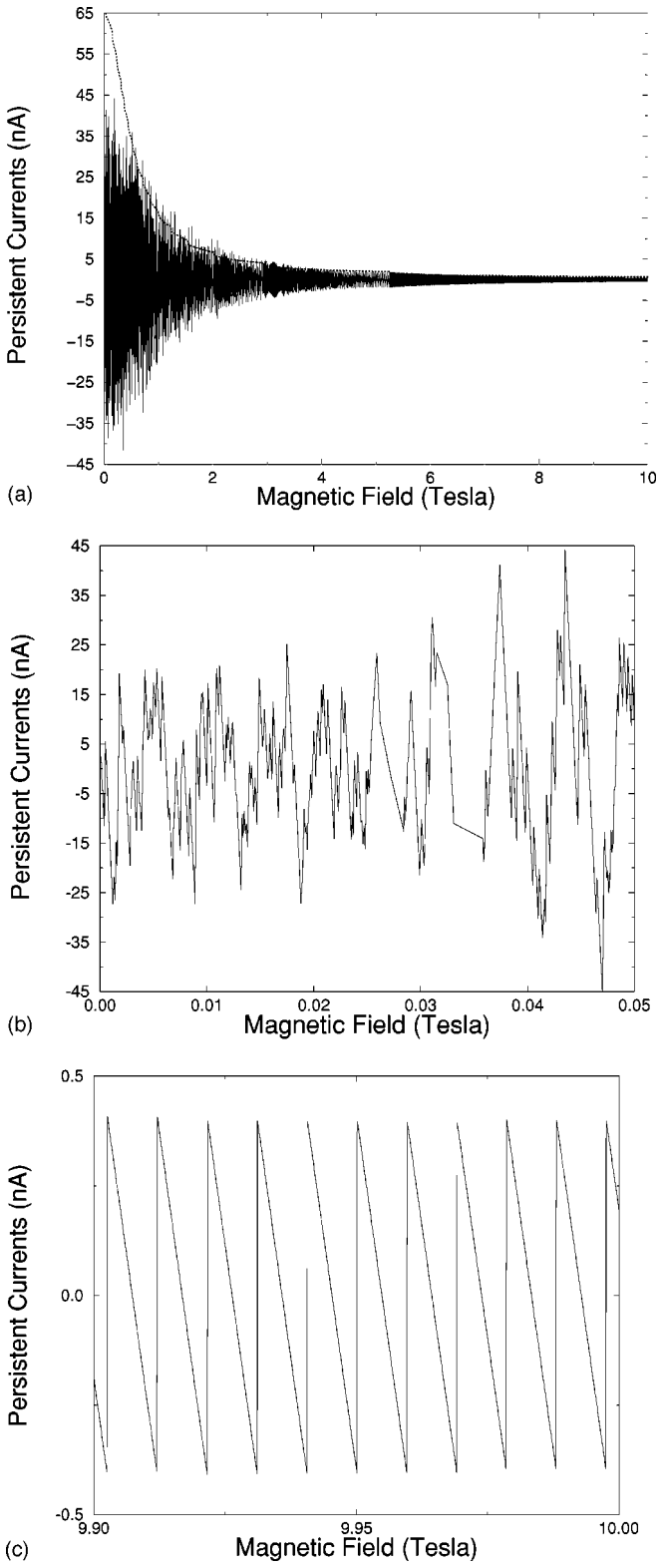

FIG. 4. (a) The persistent currents of the wide ring as a function of magnetic-field strength obtained from the exact model calculation (real line). The broken line shows the persistent currents calculated with the simple formula (19). (b) and (c) are the enlargements of the weak- and strong-field parts of (a), respectively.

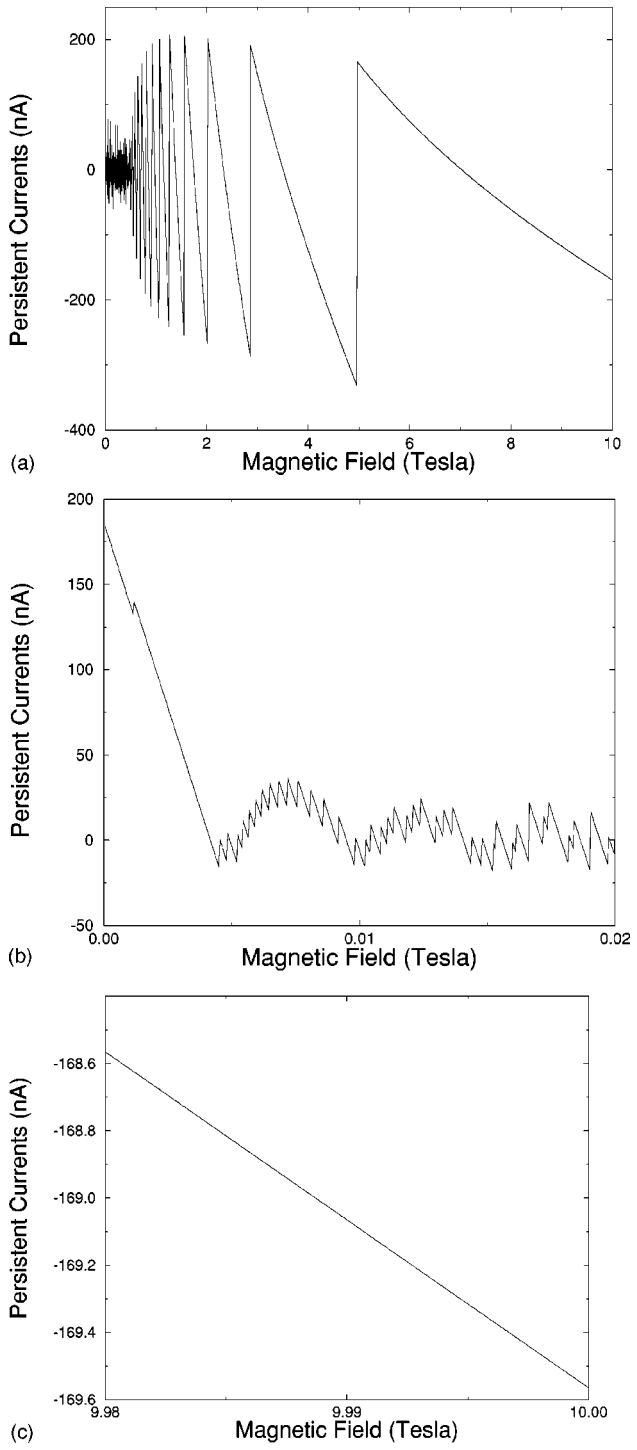

FIG. 5. (a) The persistent currents of the dot as a function of magnetic-field strength. (b) and (c) are the enlargements of the weak- and strong-field parts of the exact results shown in (a), respectively.

Clearly the condition to have periodic oscillations in a ring with a radius r_0 and a width Δr is that the magnetic flux penetrating through the conducting region of the ring is much smaller than a flux quanta, i.e., $B \ll \phi_0 (2\pi\Delta r)^{-1}$. The number of periods of such nearly periodic oscillation is then roughly given by $N_p \approx r_0/2\Delta r$. For the wide ring, $N_p < 1$, therefore there are not periodic oscillations in the weak-field region, as can be seen in Fig. 4(b). As the magnetic-field strength increases, the oscillations of the persistent currents in a 2D ring become generally aperiodic. In addition the oscillation patterns are strongly magnetic field dependent. Comparing the persistent currents shown in Figs. 3(a) and

4(a) with the Fermi energy variation in Fig. 2, we see that the depopulation of a subband always leads to a dramatic change in the oscillation patterns.

Both Figs. 3(a) and 4(a) show that the amplitudes of the persistent currents are strongly suppressed by increasing magnetic-field strength. In a perfect 2D ring, the amplitude of the total persistent current should be of the order of[10]

$$I=\sqrt{P}\,\frac{ev_F}{2\pi r_0}, \tag{18}$$

where v_F is the Fermi velocity and P the number of the transverse channels (subbands). If we assume a parabolic dispersion, v_F is then given by $v_F=\sqrt{2E_F/\bar{\mu}}$, where $\bar{\mu}$ is the circular effective mass of an electron. It was discussed in detail in Ref. 14 that an applied magnetic field will enhance the circular effective mass of the electrons in a 2D ring roughly by a factor of $1+(\omega_c/\omega_0)^2$, which is very similar to the longitudinal effective-mass enhancement by a magnetic field in a straight quantum wire.[22] The enhancement in the circular electron mass therefore leads to a decrease of group velocities of the electrons at the Fermi energy (hence the amplitude of the persistent current). The magnetic-field dependence of the persistent currents can be therefore estimated as

$$I=\sqrt{P}\frac{e\sqrt{2E_F/\mu}}{2\pi r_0\sqrt{1+(\omega_c/\omega_0)^2}}. \tag{19}$$

For a comparison with the full results, in Figs. 3(a) and 4(a) we also plot the amplitude of the persistent currents obtained from Eq. (19) (broken lines). It can be seen that Eq. (19) provides a very good description of the magnetic-field dependence of the persistent currents over the whole range of magnetic-field strength considered. However, one can also see that Eq. (19) generally overestimates the persistent current. This is because Eq. (18) is obtained with the assumption that each of the P transverse channels carries the same persistent current ($I_0=ev_F/2\pi r_0$). In reality, the persistent current carried by the nth occupied subband is given by the contribution of the last occupied level in the subband, i.e., $I_n=ev_n/2\pi r_0$, where $v_n=\sqrt{2(E_F-E_n)/\bar{\mu}}$, and E_n is the energy of the nth subband bottom. Since $v_n<v_F$ for all channels, Eq. (18) always gives an overestimated persistent current. Such an overestimation becomes significant in case of $P\gg 1$, where $v_n\ll v_F$ for many channels. For example, there is a clear discrepancy between the exact result and that from Eq. (19) in the low-field region ($B<0.1$ T) of Fig. 4(a), where $P=16$ subbands are occupied.

Although the persistent current in a 2D ring is generally aperiodic with magnetic field, it can present nearly periodic oscillations if only the lowest subband is occupied, as shown in Figs. 3(c) and 4(c). This is easy to understand. When only one subband is occupied, each abrupt change in the persistent current simply corresponds to a jump of an electron from the inner edge to the outside edge of the ring, the period of the oscillation is therefore given by the magnetic field increment related to the two successive jumps. Such a magnetic-field increment should in turn correspond to an increment in the average magnetic flux enclosed by the inner and outer edge states by a magnetic flux quanta. In fact, it can be shown from Eq. (2) that the magnetic-field-dependent period may expressed as

$$p=\left(\frac{r_0^2}{r^+r^-}\right)^2\left(1+\frac{E_f-\hbar\omega/2}{V_0}\right)p_0, \tag{20}$$

where r^- and r^+ are the radii of inner and outer edge states at the Fermi energy. Since p is a smooth function of B one would observe nearly periodic oscillations over a small range of magnetic-field strengths.

Figure 5(a) shows that the general behavior of the persistent currents in a dot is markedly different from that in a ring, reflecting the importance of the geometry effect. As discussed at the end of Sec. II, the electron states in a dot can be divided into three classes: $m>0$, $m=0$, and $m<0$. For the parabolically confined dot, different electron states in the same class carry exactly the same current. Redistribution of electron occupation within the same class therefore has no effect on the total current. This is very different from the ring geometry, where any change in the electron occupation results in an abrupt change in the total current.

In the weak magnetic region, the lateral confinement of the quantum dot is dominant. In Fig. 5(b) we see rapid AB-like oscillations in the persistent currents. At $B=0$, the electronic states in the dot are highly degenerate at the Fermi energy. A small positive magnetic field ($B\rightarrow 0^+$) can lift the degeneracy, and near the Fermi energy more electrons will occupy the states with $m>0$, which have a lower energy than the $m\leqslant 0$ states. As a result the quantum dot often presents a large value of persistent currents at a weak B [see Fig. 5(b)]. As the magnetic field increases, however, oscillations in the persistent currents become de Hass–van Alphen (dHvA) like. The abrupt changes in the oscillation of persistent currents now result from the depopulation of the $m=0$ and $m<0$ states. In the strong-magnetic-field region, only states with $m\leqslant 0$ carry a large current, and the energies of these states are always very close to a subband bottom. Hence when and only when a subband is nearly depleted does the depopulation of the $m\leqslant 0$ states occur, and thus results in a large jump in the persistent currents. Using Eqs. (16) and (17), one can easily show that the abrupt change in the persistent currents associated with the depopulation of the nth subband is approximately $(2n+1)e\omega_c/4\pi$.

It should be pointed out that the lack of rapid oscillations in the persistent current in the strong-field regime is a special result of the parabolic model. Generally different $m>0$ states in a quantum dot with a nonparabolic confinement potential carry different amounts of currents, and therefore redistribution of electron occupation with these states should result in weak but rapid oscillations in the persistent currents. This can clearly be seen in the numerical results for a hard-wall-confined disk obtained by Avishai and Kohmoto.[6] When the magnetic field is so strong that only the lowest subband ($n=0$) is occupied, varying the magnetic field can no longer alter the occupation of the electron states. As a result the persistent current becomes a smooth function of magnetic-field strength [see Fig. 5(c)].

Finally we would like to compare our calculated weak-field persistent current of the narrow ring [as shown in Fig. 1(a)] with the experimental results on a single semiconductor

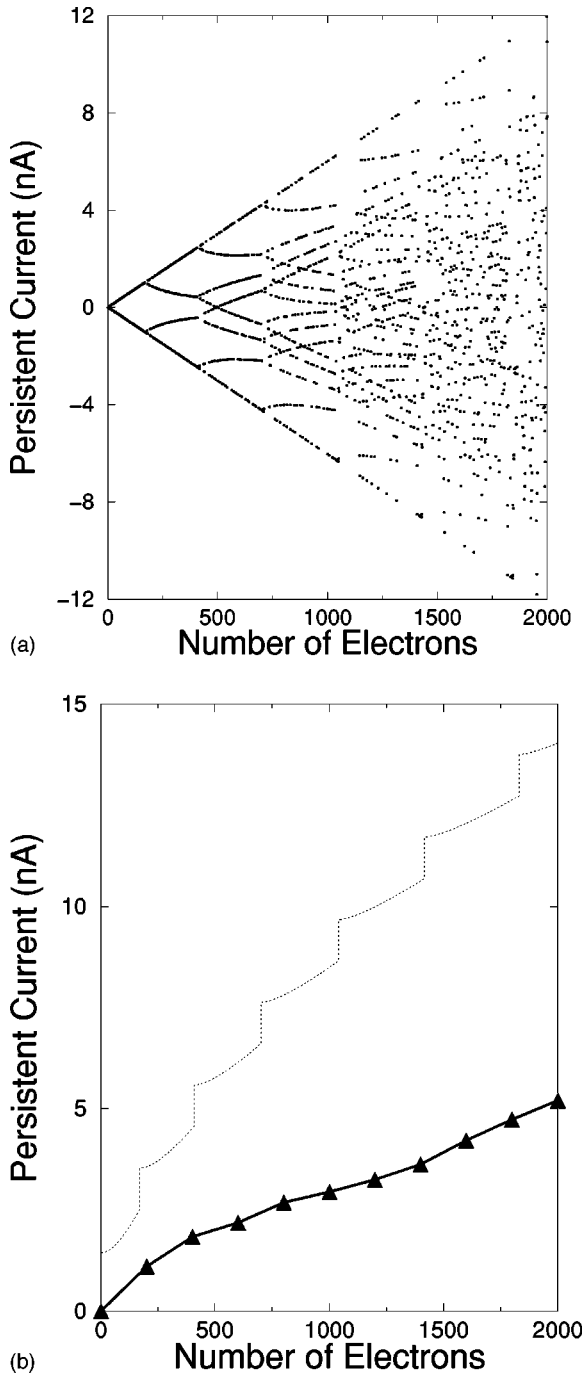

FIG. 6. (a) Persistent current vs number of (spinless) electrons in the narrow ring [as shown in Fig. 1(a)] calculated at a fix magnetic field $B=0.000\,179$ T. (b) The triangles shows the typical values of the persistent currents, i.e., the root-mean-square values of the persistent currents obtained by averaging the results shown in (a) over the electron number in an interval of 200. The broken line shows the amplitudes of persistent currents in the narrow ring obtained from Eq. (18).

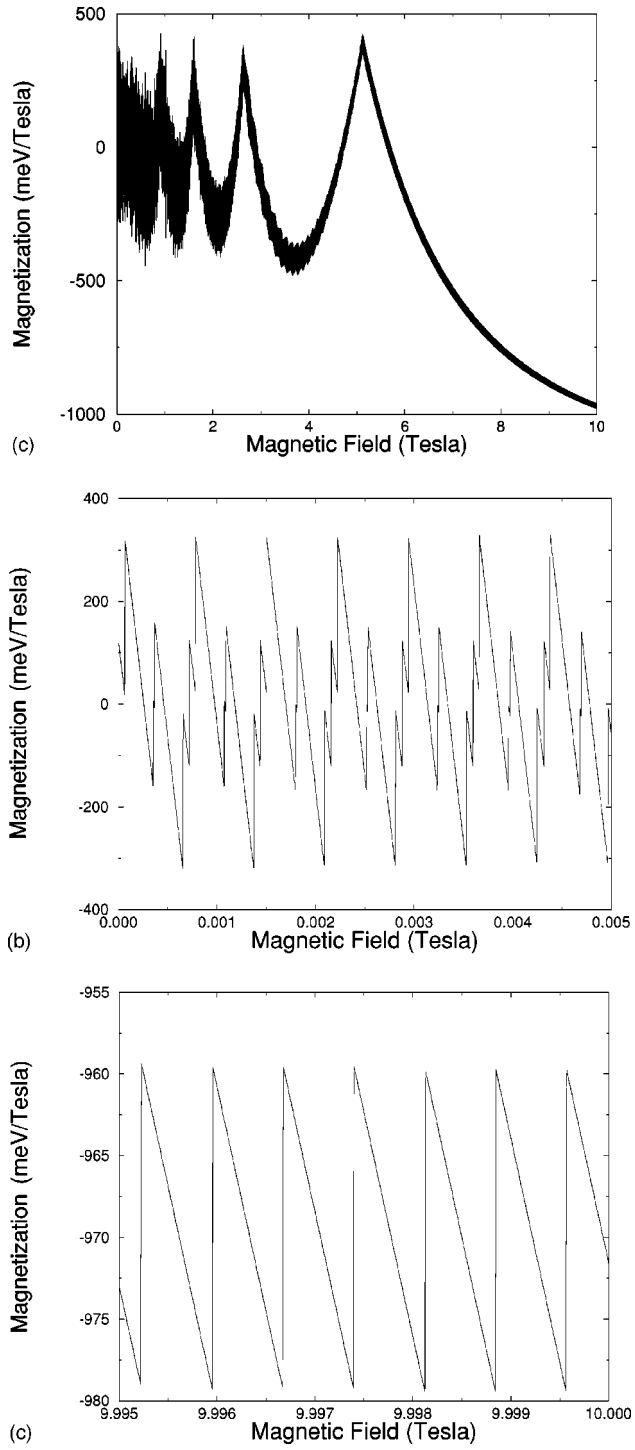

FIG. 7. (a) The magnetization of the narrow ring as a function of magnetic-field-strength. (b) and (c) are the enlargements of the weak- and strong-field parts of (a), respectively.

ring of Ref. 3. In the sample of Ref. 3, the disorder is very weak, and, ignoring interaction effects, the persistent current must be close to the value of the perfect 2D ring illustrated in Fig. 1(a). By averaging different measurements, the authors of Ref. 3 found a typical current amplitude of $I_{typ}=\langle I^2\rangle^{1/2}=4\pm2$ nA. In order to make a sensible comparison, we calculated the persistent currents for different values of electron (spinless) number (N) at a fixed magnetic field $B=0.000179$ T, at which the magnetic flux enclosed by the ring is $\phi_0/4$. The results are presented in Fig. 6(a). It can be seen that the persistent current exhibits strong oscillations as N changes. Because the subband dispersion curves in such a narrow ring are nearly parabolic,[14] the maximum possible amplitude of the persistent current is $I_{max}(N)=(N/2\pi r_0^2)(e\hbar/\mu)$. To mimic the experiment situation where the number of electrons in the ring may change in

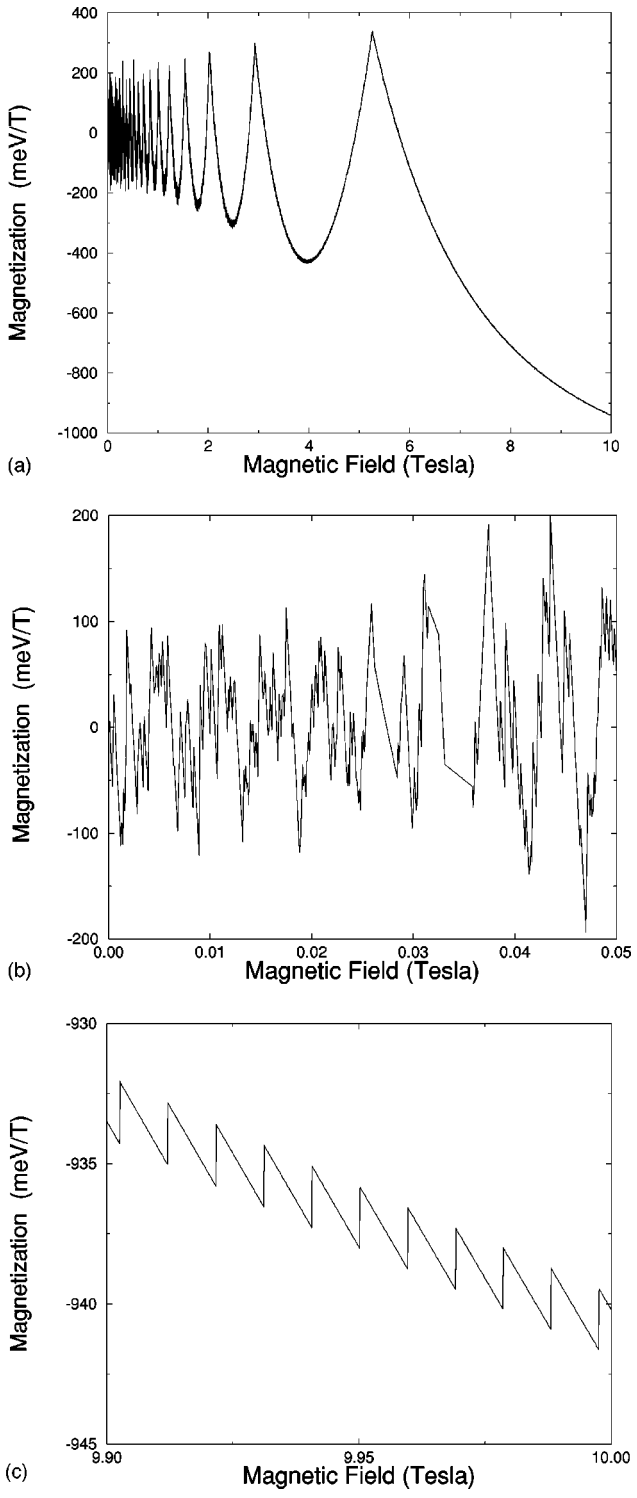

FIG. 8. (a) The magnetization of the wide ring as a function of magnetic-field strength. (b) and (c) are the enlargements of the weak- and strong-field parts of (a), respectively.

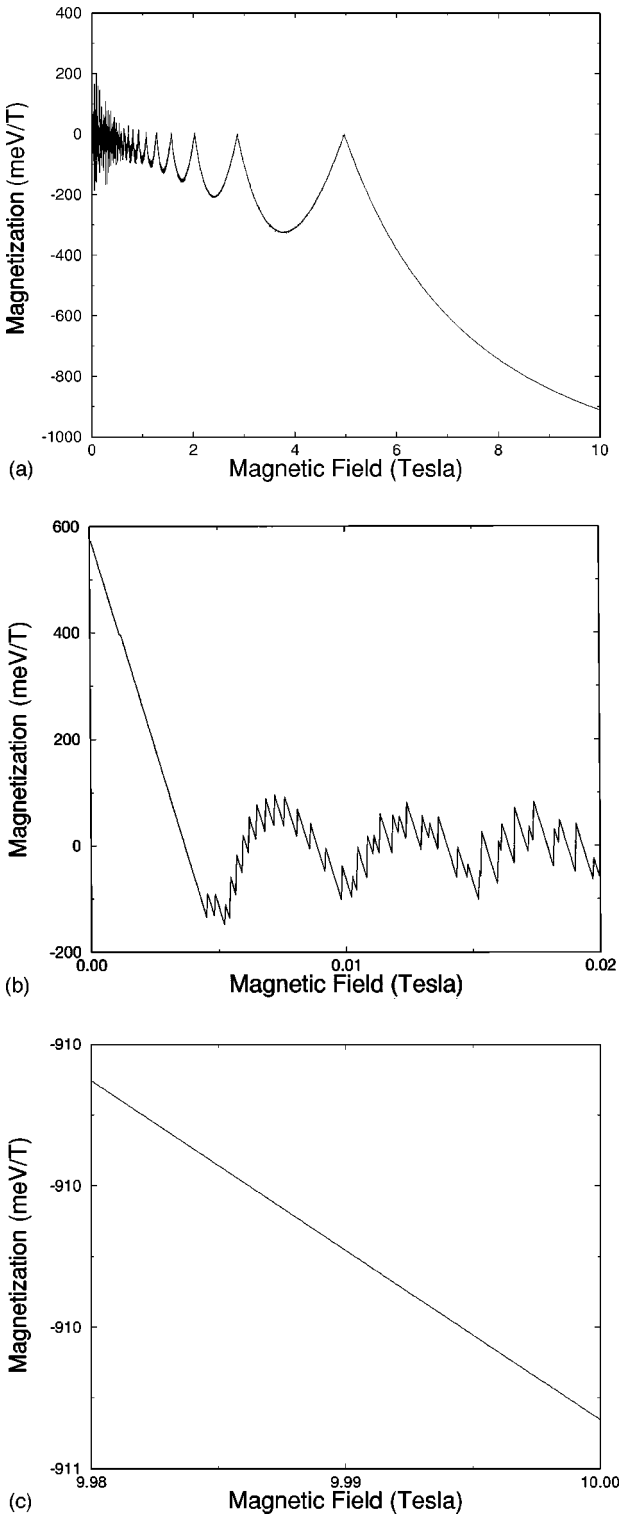

FIG. 9. (a) The magnetization of the dot as a function of magnetic-field strength. (b) and (c) are the enlargements of the weak- and strong-field parts of (a), respectively.

different measurements, we obtain the typical value of persistent current by calculating the root-mean-square of the current over the electron number in an interval of 200.[7,23] The calculated typical currents are shown in Fig. 6(b) by the line joining the calculated points (triangles). At $N \approx 1400$, which corresponds to the experimental situation, Fig. 6(b) shows that the typical value of the persistent current is $I_{typ} = 3.5$ nA. In the above discussion we have ignored the spin degree of freedom of the electrons. The spin freedom may be approximately included by multiplying a factor of $\sqrt{2}$, and then we find that the typical persistent current is $I_{typ} = 4.95$ nA. This is in very good agreement with the experimental value 4 ± 2 nA.[3]

For comparison, in Fig. 6(b) we also plot the values of persistent currents obtained from Eq. (18) (broken line). Fig-

ure 6(b) shows that the values of the persistent currents given by Eq. (18) are considerably larger than those from exact calculation. In the experiment,[3] where $N \approx 1400$ and $P=5$, we find $I_0 = ev_F/2\pi r_0 = 4.77$ nA, and therefore Eq. (18) give a typical value of persistent current $I_{typ} = \sqrt{5} I_0 = 10.6$ nA. If we again include the spin degree of freedom of the electrons by multiplying a factor of $\sqrt{2}$, we obtain $I_{typ} = 15$ nA which is significantly larger than the experimental value 4 ± 2 nA.[3] The reason for such a large overestimation has been discussed earlier in this subsection. Therefore Eq. (18) should be used with great care.

B. Magnetization

There have been several previous investigations on the magnetization and the persistent current in quantum dots. The authors of Ref. 24 studied the magnetization of a quantum dot using the parabolic confinement model in the strong-magnetic-field regime ($\omega_c \gg \omega_0$), and revealed the detailed structures in the oscillations of the magnetization. Using the same model, Yoshioka, and Fukuyama[25] studied the weak-field magnetization at zero and finite temperatures. Schult *et al.*[26] numerically investigated the magnetization in a disk with a hard-wall boundary condition, and Avishai and Kohmoto[6] studied the magnetization and persistent currents in a similar system. However, to our knowledge the persistent currents in a parabolically confined dot have not been studied before. In addition, here we provide a complete picture of magnetization in different geometries (from a narrow ring, and a wide ring to a dot), and enable a direct comparison between the magnetization and the persistent currents calculated above in these geometries.

In Figs. 7, 8, and 9 we present the calculated magnetization over a wide range of magnetic-field strength for the narrow ring, the wide ring, and the quantum dot, respectively. In the weak-magnetic-field region, the magnetization is dominated by strong mesoscopic (or AB-type) oscillations in all the three devices. The device geometry however has a significant effect on the oscillation pattern: the narrow ring exhibits periodic oscillations with the period of h/e [Fig. 7(b)], while the oscillation patterns of the wide ring and dot are clearly aperiodic [see Figs. 8(b) and 9(b)]. In addition, the quantum dot has a large positive magnetization at $B \approx 0$, which is due to the high degeneracy of the electron states in the parabolic dot.[25]

Comparing Figs. 7(b), 8(b), and 9(b) with Figs. 3(b), 4(b), and 5(b), we see that magnetization and persistent currents have a very similar low-field behavior, especially for the narrow ring. However, on the large magnetic-field-scale, magnetization is very different from persistent currents. As shown in Figs. 7(a), 8(a), and 9(a), the former is dominated by strong dHvA-type oscillations, which correspond to intersections of the Fermi energy by a Landau subband. For the two rings we can still see AB-type mesoscopic oscillations superimposed on top of the dHvA-type oscillations even in the strong-magnetic-field regime, as shown in Figs. 7(c) and 8(c), but the amplitudes of AB-type oscillations are strongly suppressed. For the dot, however, Fig. 9(c) shows there is no longer an AB-type mesoscopic oscillation when the magnetic field is so strong that only the lowest subband ($n=0$) is occupied. This is because now varying the magnetic-field strength can no longer change the occupation of the electron states in the dot. According to Eq. (9), at the limit $B \to \infty$, each electron carries a magnetic moment $\mathcal{M}_0 = -e\hbar/2\mu$, and thus the magnetization of all three devices tend to the same value $N\mathcal{M}_0$, where $N=1400$.

IV. CONCLUSIONS

We have studied the magnetization and persistent currents in mesoscopic 2D rings and dots by use of an exactly soluble model. The analytical solutions of the model allow a calculation of structures containing a large number of electrons over a wide range of magnetic-field strengths. Our results show that only in the weak-magnetic-field limit are the persistent current and the magnetization proportional to each other. In the strong-magnetic-field regime the persistent current and the magnetization have very different behaviors: the former always shows rapid AB-type oscillations, while the latter is dominated by dHvA-type oscillations with much weaker AB-type oscillations superimposed on them. It is also found that both the oscillation amplitude and the period of the persistent current are very sensitive to the device geometry, but the magnetization in different devices shows very similar dHvA-type oscillations. Our calculated typical value of low-magnetic-field persistent currents for the narrow ring, 4.95 nA, agrees very well with the experimental value, 4 ± 2 nA, for a ballistic semiconductor ring,[3] in contrast with previous theory[10] that gives an overestimated value >10 nA.

ACKNOWLEDGMENTS

The authors are grateful to the EPSRC of U.K. for supporting this research.

[1] L. P. Levy, G. Dolan, J. Dunsmuir, and H. Bouchiat, Phys. Rev. Lett. **64**, 2074 (1990).
[2] V. Chandrasekhar, R. A. Webb, M. J. Brady, M. B. Ketchen, W. J. Gallagher, and A. Kleinsasser, Phys. Rev. Lett. **67**, 3578 (1991).
[3] D. Mailly, C. Chapelier, and A. Benoit, Phys. Rev. Lett. **70**, 2020 (1993).
[4] N. Byers and C. N. Yang, Phys. Rev. Lett. **7**, 46 (1961).
[5] M. Buttiker, Y. Imry, and R. Landauer, Phys. Lett. **96A**, 365 (1983).
[6] Y. Avishai and M. Kohmoto, Phys. Rev. Lett. **71**, 279 (1993).
[7] Y. Avishai, Y. Hatsugai, and M. Kohmoto, Phys. Rev. B **47**, 9501(1993).
[8] G. Bouzerar, D. Poilblanc, and G. Montambaux, Phys. Rev. B **49**, 8258 (1994).
[9] G. Kirczenow, Superlattices Microstruct. **14**, 237 (1994); M. R. Geller and D. Loss, Phys. Rev. B **56**, 9692 (1997).
[10] H. F. Cheung, Y. Gefen, E. K. Riedel, and W. H. Shih, Phys. Rev. B **37**, 6050 (1988); H. F. Cheung, E. K. Riedel, and Y. Gefen, Phys. Rev. Lett. **62**, 587 (1989).

[11] G. Montambaux, H. Bouchiat, D. Sigeti, and R. Friesner, Phys. Rev. B **42**, 7647 (1990).
[12] D. Eliyahu, R. Berkovits, M. Abraham, and Y. Avishai, Phys. Rev. B **49**, 14 448 (1994).
[13] T. Chakraborty and P. Pietilainen, Phys. Rev. B **50**, 8460 (1994).
[14] W.-C. Tan and J. C. Inkson, Semicond. Sci. Technol. **11**, 1635 (1996).
[15] W.-C. Tan and J. C. Inkson, Phys. Rev. B **53**, 6947 (1996).
[16] J. Liu, W. X. Gao, K. Ismail, K. Y. Lee, J. M. Hong, and S. Washburn, Phys. Rev. B **48**, 15 148 (1993).
[17] A. A. Bykov, Z. D. Kvon, and E. B. Olshanetskii, Inst. Phys. Conf. Ser. **145**, 909 (1996).
[18] M. M. Fogler, E. I. Levin, and B. I. Shklovskii, Phys. Rev. B **49**, 13 767 (1994).
[19] P. Hawrylak, Phys. Rev. Lett. **71**, 3347 (1993).
[20] P. L. McEuen, E. B. Foxman, J. Kinaret, U. Meirav, M. Kastner, N. S. Wingreen, and S. J. Wind, Phys. Rev. B **45**, 11 419 (1992); R. C. Ashoori, H. L. Stormer, J. S. Weiner, L. N. Pfeiffer, K. Baldwin, and K. W West, Phys. Rev. Lett. **71**, 613 (1993); N. F. Johnson and L. Quiroga, J. Phys.: Condens. Matter **9**, 5889 (1997).
[21] V. Ambegaokar and U. Eckern, Phys. Rev. Lett. **65**, 381 (1990); A. Schmid, *ibid.* **66**, 80 (1991); P. Kopietz, *ibid.* **70**, 3123 (1993); D. Loss, *ibid.* **69**, 343 (1993); R. Berkovits and Y. Avishai, *ibid.* **76**, 291 (1996).
[22] K.-F. Berggren, T. J. Thornton, D. J. Newson, and M. Pepper, Phys. Rev. Lett. **57**, 1769 (1986); W.-C Tan, J. C. Inkson, and G. P. Srivastava, Semicond. Sci. Technol. **9**, 1305 (1994).
[23] R. A. Jalabert, Surf. Sci. **362**, 700 (1996).
[24] Y. Meir, O. Entin-Wohlman, and Y. Gefen, Phys. Rev. B **42**, 8351 (1990).
[25] D. Yoshioka and H. Fukuyama, J. Phys. Soc. Jpn. **61**, 2368 (1992).
[26] R. L. Schult, M. Stone, H. W. Wyld, and D. G. Ravenhall, Superlattices Microstruct. **11**, 73 (1992).